Mechanical Interaction Between the Tendons of the Extrinsic Finger Flexors

Maas, H.; Geusebroek, G.; Baan, G. C.; Veeger, H. E.J.

DOI
10.1111/sms.14682

Publication date
2024

Document Version
Final published version

Published in
Scandinavian Journal of Medicine and Science in Sports

Citation (APA)
Maas, H., Geusebroek, G., Baan, G. C., & Veeger, H. E. J. (2024). Mechanical Interaction Between the Tendons of the Extrinsic Finger Flexors. *Scandinavian Journal of Medicine and Science in Sports*, *34*(6), Article e14682. https://doi.org/10.1111/sms.14682

Scandinavian Journal of Medicine & Science in Sports

WILEY

ORIGINAL ARTICLE OPEN ACCESS

Mechanical Interaction Between the Tendons of the Extrinsic Finger Flexors

H. Maas[1] | G. Geusebroek[1] | G. C. Baan[1] | H. E. J. Veeger[2]

[1]Department of Human Movement Sciences, Faculty of Behavioural and Movement Sciences, Vrije Universiteit Amsterdam, Amsterdam Movement Sciences, Amsterdam, The Netherlands | [2]Department of Biomechanical Engineering, Delft University of Technology, Delft, The Netherlands

Correspondence: H. Maas (h.maas@vu.nl)

Received: 7 February 2024 | **Revised:** 30 April 2024 | **Accepted:** 2 June 2024

Funding: The authors received no specific funding for this work.

Keywords: connective tissue | dexterity | finger enslaving | flexor digitorum profundus | flexor digitorum superficialis | range of independent movement | tendon

ABSTRACT

Humans possess an incredible capacity for dexterity, but independent finger control is limited. One factor constraining finger independence is the connections between the tendons of the extrinsic finger muscles. The aim of this study was to assess to what extent the linkages between the distal tendons of flexor digitorum profundus (FDP) and those of the flexor digitorum superficialis (FDS) constrain finger independence. Experiments on human fresh frozen cadaveric upper extremities ($n=6$) were performed. First, one finger (target) was flexed whereas the other (nontarget) fingers were held in a nearly extended position. The change (Δ) in total flexion angle ($\sum\Theta$; i.e., the sum of angles of the different finger joints) of the target finger from the $\sum\Theta$ corresponding to the extended position at the start of the movement until the $\sum\Theta$ corresponding to the onset of force exertion at the nontarget fingers was assessed. Second, the distribution of force across the four fingers upon loading the tendon of the target finger was assessed for two finger positions (extended, 90° flexion of metacarpal phalangeal joint). For both muscles and for all fingers, the range of independent movement was small (<7°). $\Delta\sum\Theta$ at force onset was lowest for fingers immediately adjacent to the target finger and highest for more distant fingers. For both muscles and for all fingers, some of the target finger force (<14% for FDP, <2% for FDS) was distributed to the nontarget fingers, which increased (up to 58%) only for FDP in response to target finger flexion. We conclude that mechanical connections between the FDP and FDS tendons constrain finger independence. Such constraints become apparent when moving one finger relative to the other fingers.

1 | Introduction

Humans possess an incredible capacity for dexterity. We use our hands for a large variety of daily tasks, such as writing and tying shoelaces, but also for more specialized tasks requiring fine finger movements, such as playing a musical instrument. It may seem that the possibilities are unlimited, but that is not the case. When asked to move a single finger, after some independent movement [1] the other fingers start moving unintentionally as well [2–4]. Also, in a force producing task, fingers cannot exert force independently [5–8]. In the past, the cause for this interdependency has been labeled neurological as well as mechanical [9, 10].

Finger movements are controlled by intrinsic and extrinsic muscles. The main extrinsic muscles are the extensor digitorum (ED), the flexor digitorum profundus (FDP), and the flexor digitorum superficialis (FDS). For all the extrinsic finger extensors and flexors, connections between the tendons of each muscle have been described [11–15]. However, experimental studies assessing the mechanical consequences of these linkages are scarce. Cadaver studies in which the intertendinous connective tissue of the ED and the interfinger web were sequentially disrupted showed that the interaction between fingers decreased [12]. Using a model of two heads of the FDP and a stiffness between the tendons, it was demonstrated that finger interdependence may be caused by intertendinous connections [16]. In addition, Leijnse described a single case study in which surgically removing all connections between the FDP tendons resulted in improved finger independence.

The aim of the present exploratory study was to assess to what extent the linkages between the distal tendons of FDP and those of FDS mechanically constrain finger independence. For this purpose, experiments on human cadaveric upper extremities were performed to assess the range of independent movement for each finger and the distribution of force exerted on a single tendon proximally, across the four tendons distally, for two relative finger positions. On the basis of our previous study in which a range of independent movement was identified for each finger [1], we hypothesized a similar independent range for the intertendinous linkages. In agreement with other results from our laboratory [7], we further predicted that moving one finger relative to the other fingers will tauten the intertendinous connections and, hence, more force will be transmitted to the neighboring fingers.

2 | Methods

2.1 | Specimen Preparation

Six fresh frozen cadaveric right arms were used for the experiments, as approved by the Biobank Review Committee of the Vrije Universiteit Medical Center (2017.098). All donors were male (mean age: 78.2 ± 15.6 years). We selected males to limit the potential effects of osteoporosis, which would cause problems with the application of bone screws. One donor suffered from arthritis and another from a transient ischemic attack which affected hand function. However, no restrictions in finger movements were observed in the specimen. The hand and lower arm were amputated approximately 10 cm proximal of the wrist. The volar forearm skin was removed up to the pisiform bone at the ulnar side and up to the tubercle of scaphoid bone at the radial side. If present, the tendon of the palmaris longus was cut near the wrist. The muscle bellies of FDP and FDS were cut from their respective distal tendons. For each of the FDP and FDS tendons, the corresponding finger was identified. A polyester sewing thread was sutured on the proximal ends of the tendons so that a load could be attached. To prevent dehydration of the exposed tissues, a saline solution was applied regularly.

The lower arm was mounted in a frame (Figure 1) by two parallel pins (ø = 3.0 mm), both penetrating radius and ulna 5–10 cm apart. The wrist was fixed in a standard position (≈20° dorsiflexion) by a custom-built external wrist fixator, which was secured to the radio-dorsal side of the radius with two Schanz-screws (ø = 2.5 mm) and to the dorsal side of the hand with three Schanz screws (ø = 2.5 mm) drilled in the second, third, and fourth metacarpal bone. The hand was secured to the setup by two threaded pins (ø = 2.5 mm) drilled in the base of the radial side of the second and the ulnar side of the fifth metacarpal bone.

Stainless steel bone screws (ø = 2.0 mm) were secured to the dorsal aspect of the distal and intermediate phalanx of the four fingers (i.e., digits II–V), using similar procedures as described previously [17]. The screws were used to attach clusters with three active markers (Optotrak, Northern Digital Inc., Canada), as well as steel wires (ø = 1.0 mm) for connecting the dorsal side of the fingers to force transducers (FUTEK miniature S-Beam JR load cell, model LSB200, capacity 10 lb, nonlinearity ±0.1%, sensitivity 2 mV/V) mounted in the frame. Another cluster was secured to the second metacarpal bone.

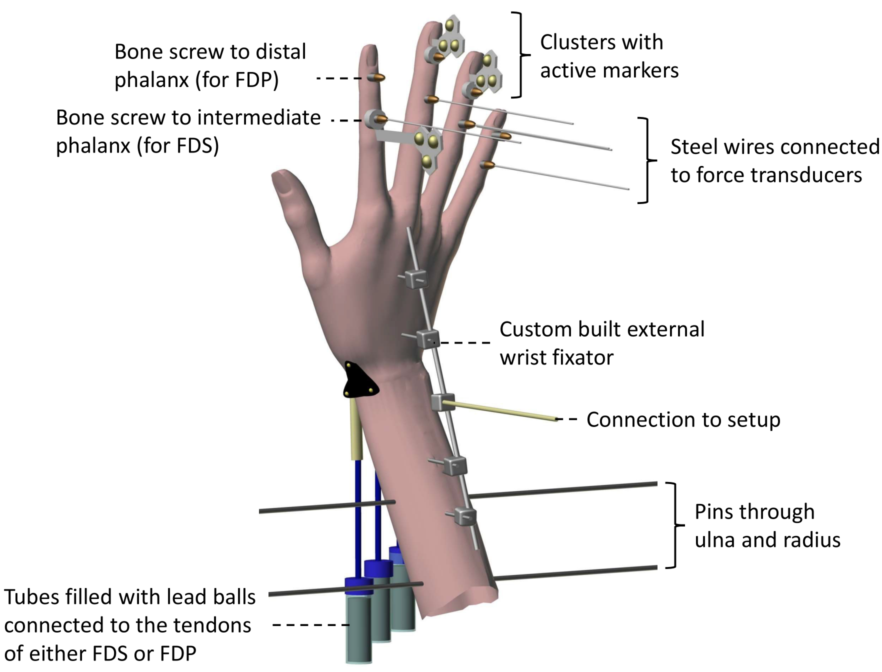

FIGURE 1 | Schematic view of the specimen in the experimental setup (for details, see main text). Drawing made by G.C. Baan using Anim8or.

2.2 | Data Collection

Three dimensional positions of the markers in an orthogonal global coordinate system were recorded by two Optotrak cameras (Optotrak Certus 3020, Northern Digital Inc., Canada) with a sample frequency of 50 Hz. Force transducers were connected to an ADC (Porti 8, 24 bits resolution for AUX channels, effective resolution 1.6 mN/bit; TMSI, Enschede, Netherlands), and force signals were sampled at 500 Hz. Marker position and force signals were synchronized by a trigger pulse sent at the initiation of motion tracking, using the external sync port of the system control unit of the Optotrak to the ADC.

2.3 | Experimental Protocols

Two experimental protocols were performed: Protocol A to assess the range of independent movement and Protocol B to assess the distribution of a proximally applied force on one tendon across the four fingers.

2.3.1 | Protocol A

By attaching a 3 N weight (i.e., a tube filled with lead balls) to the proximal tendon ends, a constant load was applied to the four proximal tendons of either FDS or FDP. The 3 N weight was an arbitrary value, based on pilot experiments. All fingers, except for the target finger, were held in a nearly extended position (i.e., ≈0° for the metacarpal phalangeal joint—MCP, ≈30° for the proximal interphalangeal joint—PIP and ≈20° for the distal interphalangeal joint—DIP) by their attachment to the force transducers. As the insertions of the FDP tendons are on the distal phalanges, the force transducers were linked to the distal phalanges when measuring mechanical interactions between the FDP tendons. Similarly, the force transducers were linked to the intermediate phalanges when measuring the FDS. The connected phalanges were oriented orthogonally to the line of pull of the force transducers. The target finger was detached from the force transducer and manually guided in a slow flexion movement caused by the 3 N load until maximal finger flexion followed by finger extension. This movement was performed three times for each finger in a fixed order (i.e., index, ring, middle, and little finger). After all fingers were completed with loading the tendons of the FDP, the weights were replaced to the tendons of FDS and the protocol was repeated.

2.3.2 | Protocol B

In a similar way as in Protocol A, a constant load was applied to the four distal tendons of either FDS or FDP. To assess if moving one finger relative to the other fingers will tauten the intertendinous connections and, hence, more force will be transmitted to the neighboring fingers, two positions of the target finger were tested. With the fingers held in the "natural" extended position, described above, a 3 N load was applied to the tendons corresponding to the nontarget fingers and a 10 N load was applied to the tendon corresponding to the target finger for ≈5 s. Subsequently, the MCP joint of the target finger was flexed by 90° and the 10 N load was applied for another ≈5 s. This procedure was repeated for each FDS tendon and after replacing the weights for each FDP tendon. A somewhat larger weight (10 N) was selected to allow for accurate assessments of the transmission of low forces to neighboring fingers.

2.4 | Data Analysis

All data analysis was performed using MATLAB (version R2015b, MathWorks). For the data collected in Protocol A, MCP, PIP, and DIP joint angles were assessed using a linked-segment-model, adapted from Mirakhorlo et al. [17]. This model consists of four rigid bodies per finger (i.e., one metacarpal bone and three phalanges), seven bony landmarks per finger (i.e., fingertip, ulnar and radial aspect of DIP and PIP, dorsal aspect of MCP and dorsal aspect of metacarpal base) and four rigid bodies for the hand (i.e., ulnar aspect of the fifth and radial aspect of the second MCP, ulnar and radial styloid). In a reference measurement with the hand including cluster markers positioned palm down on a table, these landmarks were digitized in the global coordinate system using a custom-built, four-marker pointer with a sharp tip. Each bony landmark (BLM) was computed in the local coordinate system of its respective cluster. Subsequently, the BLM coordinates were transformed back to the global coordinate system for assessment of joint angles.

Next step was to calculate the middle of the axis for the DIP, PIP, MCP, and carpometacarpal (CMC) joints, which are needed to define the hand model (Figure 2). For the DIP and PIP joints, the middle of the joint axis was defined as the middle of the vectors from the ulnar to radial aspect of each joint. For the MCP joints, the middle of the joint axis was assessed by calculating a plane with the cross-product of two vectors both originating from the center of the line between the ulnar and radial styloid. One vector is directed toward the ulnar aspect of the fifth MCP joint, the other toward the radial aspect of the second MCP joint. The middle of MCP axis was defined as the point where the vector through the dorsal aspect of the MCP (BLM) perpendicular to this plane crosses that plane. The middle of the axis of the CMC joints was assessed by first calculating a plane using the cross-product of two vectors, both originating from the center of the line between the ulnar aspect of the fifth MCP and the radial aspect of second MCP. One vector is directed toward the ulnar styloid, the other toward the radial styloid. The middle of the CMC axis was defined in a similar way as for the MCP, but now using the vector through the dorsal aspect of the proximal endo of the metacarpal bone. Subsequently, vectors between the middle of the joint axes defined the four rigid bodies in each finger. These rigid bodies were used to calculate DIP, PIP, and MCP joint angles. For the DIP and PIP joints, the angles were calculated as the angles between the corresponding vectors, whereas for the MCP joint, the angles were calculated as the angle of the corresponding vectors projected in the sagittal plane, ignoring the MCP ad- and abduction angles. When cluster markers were occluded, joint angles were interpolated with a third order polynomial piecewise cubic Hermite spline and lowpass filtered at 2 Hz with a fourth order, zero-lag Butterworth filter. The total flexion angle ($\sum\Theta$) was calculated by summing the angles of the different joints within each finger (i.e., MCP, PIP, and DIP joint angles in case of FDP; MCP and PIP in case of FDS). The change in total flexion angle ($\Delta\sum\Theta$) of the target finger from the $\sum\Theta$

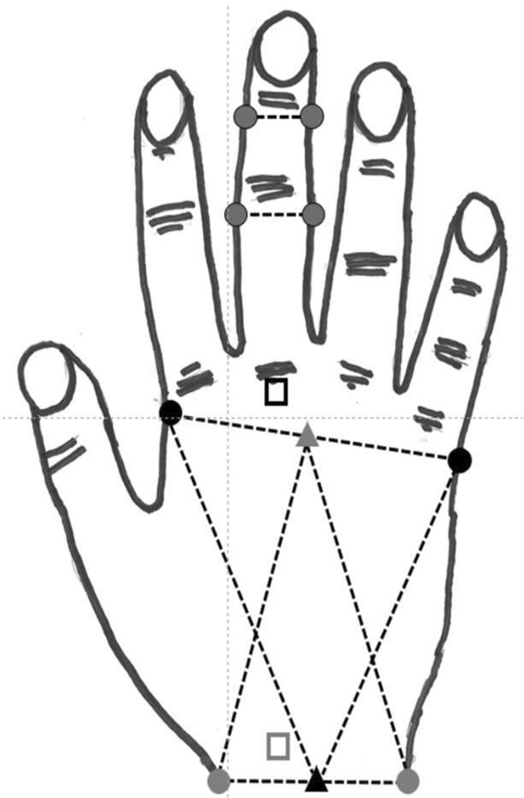

FIGURE 2 | The bony landmarks for one finger (middle) and vectors that were used to define the kinematic hand model. For the proximal interphalangeal and the distal interphalangeal joints, the middle of the joint axis was defined as the middle of the vectors from the ulnar to radial aspect of each joint (circles on middle finger). For the MCP joints, the middle of the joint axis was assessed by calculating a plane with the cross-product of two vectors both originating from the center of the line between the ulnar and radial styloid (black triangle). One vector is directed toward the ulnar aspect of the fifth MCP joint, the other toward the radial aspect of the second MCP joint (black circles). The middle of MCP axis was defined as the point where the vector through the dorsal aspect of the MCP (BLM) perpendicular to this plane crosses that plane (black square). The middle of the axis of the carpometacarpal (CMC) joints was assessed by first calculating a plane using the cross-product of two vectors, both originating from the center of the line between the ulnar aspect of the fifth MCP and the radial aspect of second MCP (gray triangle). One vector is directed toward the ulnar styloid, the other toward the radial styloid (gray circles). The middle of the CMC axis was defined in a similar way as for the MCP, but now using the vector through the dorsal aspect of the proximal endo of the metacarpal bone (gray square).

corresponding to the extended position at the start of the movement until the $\sum\Theta$ corresponding to the onset of force exertion at the nontarget fingers was assessed.

All force signals were lowpass filtered at 2 Hz with a fourth order, zero-lag Butterworth filter. For the analysis of data collected in Protocol A (Figure 3A), force signals were downsampled to the sampling frequency of the motion capture data system (50 Hz). First, the onset of flexion of the target finger, observed as a clear uninterrupted increase in $\Delta\sum\Theta$, was identified by eye. Then, the time derivative of the force signals of the nontarget fingers was calculated. The first positive value of this time derivative after the onset of target-finger flexion was defined as the onset of force exertion. If no increase in force was detected, force onset was set to the maximal $\Delta\sum\Theta$. The range of independent movement was defined as the smallest $\Delta\sum\Theta$ across all nontarget fingers.

For the data collected in Protocol B (Figure 3B), the change in force (ΔF) upon exertion of the 10 N load was calculated for each finger by subtracting the mean force of the 2 s before loading from the mean of 2 s during the loading after peak force was reached. For each of the nontarget fingers, the relative force change was calculated as:

$$\text{relative force change} = \left(\Delta F_{\text{nontarget}} / \sum \Delta F_{\text{all-fingers}}\right) \times 100\,\%$$

2.5 | Statistical Analysis

All statistical analyses were performed using Jamovi (version 2.3.2). In some cases, during ring finger and little finger movements, not all markers were visible and $\Delta\sum\Theta$ could not be calculated. This led to the exclusion of two data sets for movement of the ring finger and one for the little finger during FDP loading and one for movement of the little finger during FDS loading, reducing the number of samples for statistical analysis.

As for small sample sizes, normality tests have little power [18], we assumed that the sample was drawn from a normally distributed population. To test if the range of independent movement differed between fingers, one-way ANOVAs were performed for each muscle. To test for differences between the nontarget fingers regarding the $\Delta\sum\Theta$ at force onset, one-way ANOVAs were performed for each target finger within in each muscle. If a significant effect was found, Tukey post hoc tests were performed. To test for effects of target finger position (extended vs. 90° MCP flexion) on the relative force exerted by nontarget fingers, two-way mixed ANOVAs were performed for each target finger within each muscle. In case of significant interaction effects, Tukey post hoc tests were performed. The significance threshold was set at $p = 0.05$.

3 | Results

3.1 | Protocol A—Range of Independent Movement

For both muscles and for all fingers, the range of independent movement was small ($\Delta\sum\Theta \leq 7°$; Figures 4 and 5, see Appendix S1 for the individual data). For the FDP, the range of independent movement of the index, middle, ring, and little fingers was $7.0 \pm 13.3°$ (mean ± SD), $1.7 \pm 1.5°$, $1.3 \pm 0.5°$, and $1.3 \pm 1.4°$, respectively. For the FDS, this was $1.1 \pm 0.9°$, $0.2 \pm 0.12°$, $0.3 \pm 0.2°$, and $0.5 \pm 0.5°$ for index, middle, ring, and little fingers, respectively. For both FDP and FDS, no significant differences in range of independent movement between target fingers were found (FDP—$F = 0.438$, $p = 0.732$; FDS—$F = 2.715$, $p = 0.107$).

For both FDP and FDS, differences in $\Delta\sum\Theta$ at force onset between the nontarget fingers were observed (see Table 1 for p-values; see Appendix S2 for the individual data). In general, the $\Delta\sum\Theta$ at force onset was lowest for the fingers immediately

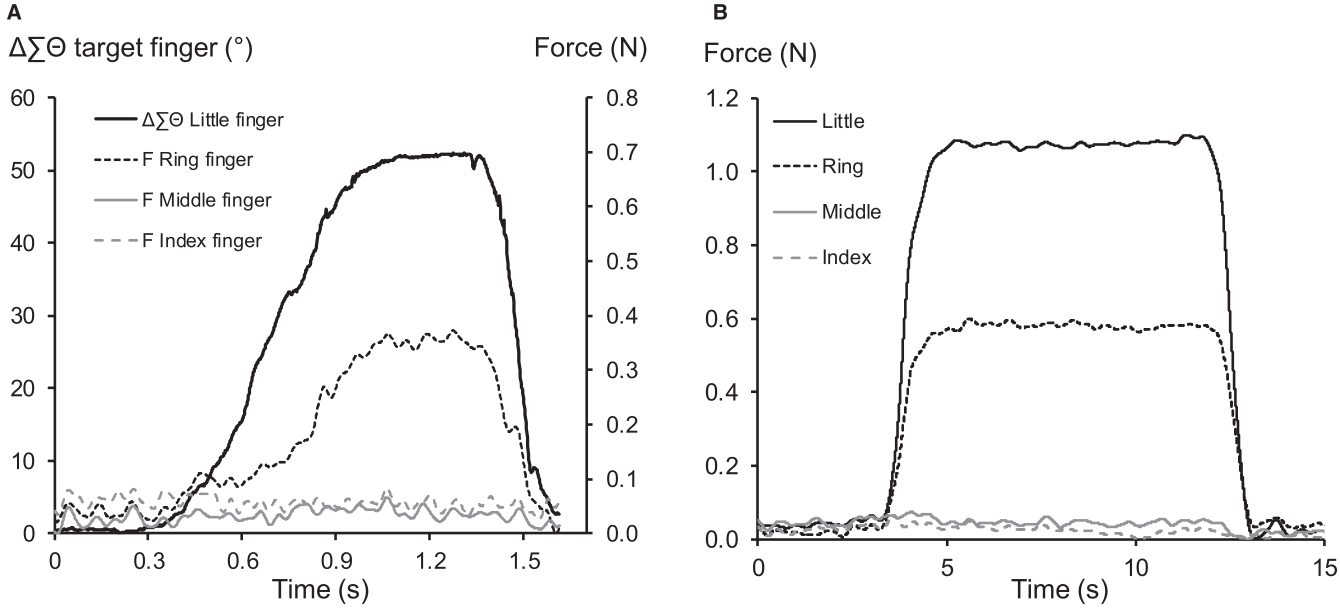

FIGURE 3 | Exemplar waveforms of data collected during protocol A (left) and B (right). In both cases, the little finger was the target finger and the flexor digitorum profundus (FDP) tendons were loaded. On the left, it is shown that flexing (ΔΣΘ) the little finger results in an almost immediate increase in force (F) exerted at the ring finger. Variability in finger forces was partly caused by the manual guiding of the target finger. On the right, the changes in force upon exertion of the 10 N load on the tendon of the little finger were measured for the condition in which its MCP joint was flexed by 90°. Note that a substantial portion of the force was distributed to the adjacent ring finger, but not to the other nontarget fingers.

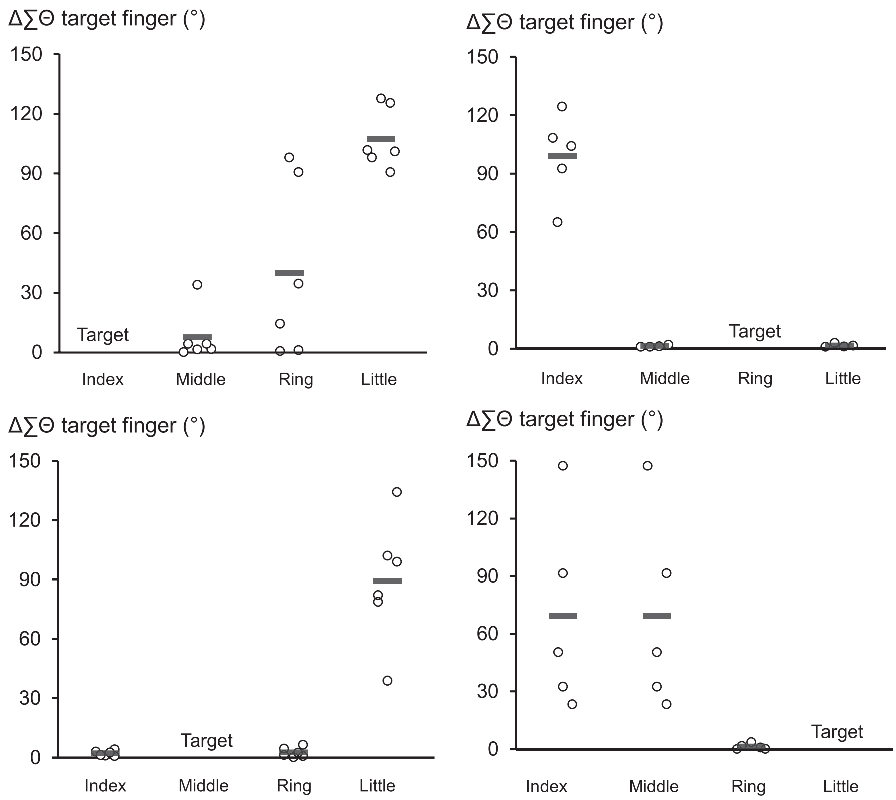

FIGURE 4 | Change in target finger flexion until onset of force exertion at the nontarget fingers during loading of the flexor digitorum profundus tendons. The individual values (n = 4, 5 or 6) and the mean are shown. The change in total flexion angle (ΔΣΘ) was calculated by summing the angles of the different joints. If no increase in force at the tendon was detected, force onset was set to the maximal ΔΣΘ. Maximal ΔΣΘ was 108 ± 15° (mean ± SD), 89 ± 32°, 99 ± 22°, and 106 ± 51° for index, middle, ring, and little fingers, respectively (see Appendix S3 for individual data). For results of post hoc analysis to test for difference between nontarget fingers, see Table 1.

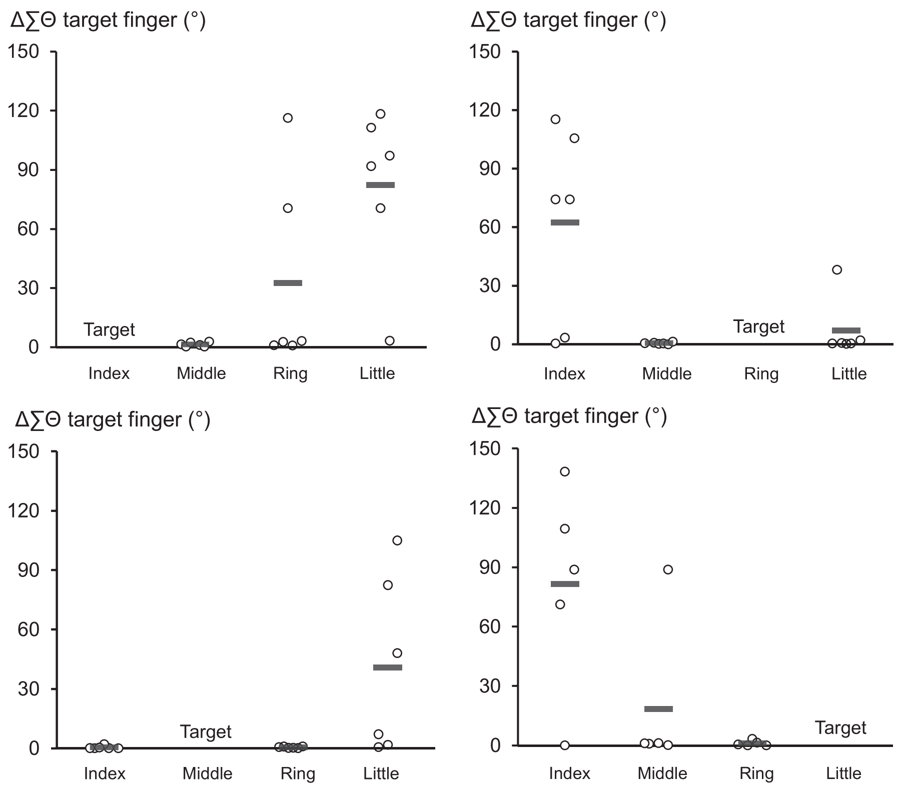

FIGURE 5 | Change in target finger flexion until onset of force exertion at the nontarget fingers during loading of the flexor digitorum superficialis tendons. The individual values ($n=5$ or 6) and the mean are shown. The change in total flexion angle (ΔΣΘ) was calculated by summing the angles of the different joints. If no increase in force at the tendon was detected, force onset was set to the maximal ΔΣΘ. Maximal ΔΣΘ was 101 ± 18° (mean ± SD), 103 ± 17°, 103 ± 24°, and 103 ± 25° for index, middle, ring, and little fingers, respectively (see Appendix S3 for individual data). For results of post hoc analysis to test for difference between nontarget fingers, see Table 1.

TABLE 1 | F and p values of one-way ANOVAs and Tukey post hoc tests to test for differences in targeted finger flexion angle (ΔΣΘ-F) at force onset by a nontarget finger (NTF).

			Index		Middle		Ring		Little	
			F	***p***	***F***	***p***	***F***	***p***	***F***	***p***
FDP	ΔΣΘ-*F*	NTF	**68.9**	**<0.001**	**21.1**	**<0.001**	**43.6**	**<0.001**	**7.8**	**0.026**
	Post hoc	Index-middle		—		—		**<0.001**		1.000
		Index-ring		—		0.999		—		0.059
		Index-little		—		**<0.001**		**<0.001**		—
		Middle-ring		0.146		—		—		0.059
		Middle-little		**<0.001**		—		0.999		—
		Ring-little		**0.002**		**<0.001**		—		—
FDS	ΔΣΘ-F	NTF	**11.1**	**0.008**	2.21	0.170	4.7	0.053	**5.8**	**0.046**
	Post hoc	Index-middle		—		—		—		0.051
		Index-ring		—		—		—		**0.014**
		Index-little		—		—		—		—
		Middle-ring		0.349		—		—		0.752
		Middle-little		**0.005**		—		—		—
		Ring-little		0.087		—		—		—

Note: Analysis has been done for each target finger (index, middle, ring, and little fingers) and flexor digitorum profundus (FDP) and superficialis (FDS) separately. A bold font depicts a significant effect ($p < 0.05$).

adjacent to the target finger and highest for the more distant fingers (Figures 4 and 5). For FDP, several more distant fingers did not exert any force during target finger flexion. For FDS, a force was exerted by all nontarget fingers at some point during flexion of the target finger. For several cases, force onset occurred at a lower total flexion angle ($\Delta\Sigma\Theta$) of the target finger in immediately adjacent fingers than in the more distant fingers. These results indicate that the intertendinous linkages of FDP and FDS transmit forces almost immediately when moving a single finger and, thereby, act as a constraint for finger independence.

3.2 | Protocol B—Distribution of Forces

For both muscles and all fingers, some of the force (up to 14% for the FDP and up to 2% for the FDS in the extended finger position) exerted on the tendon corresponding to the target finger was distributed to the nontarget fingers (Figures 6 and 7, See Appendix S4 for the individual data). For loading the FDP tendons of the middle and little fingers, two-way mixed ANOVAs indicated a significant interaction between nontarget finger and target finger position (Table 2). A significant increase in relative force was found for only the ring finger in response to flexion of the middle ($p = 0.047$; from 3% to 29%) and little fingers ($p < 0.001$, from 14% to 58%; Figure 6). No significant interactions were found for the conditions in which the FDS tendons were loaded. However, a significant main effect of target finger position was found for FDS when loading the ring finger (Table 2, Figure 7). These results indicate that intertendinous connections between some of the FDP and FDS tendons transmit forces and that the extent of such force transmission is increased when moving one finger relative to the other fingers.

4 | Discussion

Independent finger control is limited, which is mediated by neural and musculoskeletal mechanisms [9, 10]. Regarding the musculoskeletal mechanisms, several candidates have been described: (i) the complex anatomy of the extrinsic muscles actuating the fingers, such as a muscle compartment arranged in series with multiple distal tendons of the FDS muscle [10, 19, 20]; (ii) myofascial force transmission, that is, transmission of forces from a muscle compartment of one finger to a muscle compartment of a neighboring finger [21, 22]; and (iii) force transmission via connective tissue linkages between the tendons of extrinsic finger muscles and the soft tissue web between the fingers [11–15]. In this study, we investigated the functional consequences of the connective tissue linkages between the tendons of FDP and FDS muscles in the human hand. In contrast to our hypothesis, the range of independent movement as assessed by the onset of forces exerted by one of the nontarget fingers was much lower and in some cases even almost absent compared with observations during voluntary single finger movements [1]. Our results are in agreement with our second hypothesis that more force will be transmitted to the neighboring tendons in the condition in which one finger is moved relative to the other fingers.

4.1 | Range of Independent Movement

When moving a single finger in the present study (Protocol A), forces were observed in the nontarget fingers after very small movements of the target finger; that is, a maximal $\Delta\Sigma\Theta$ of 7° found for the index finger during FDP tendon loading. In agreement with this finding, immediate movements of

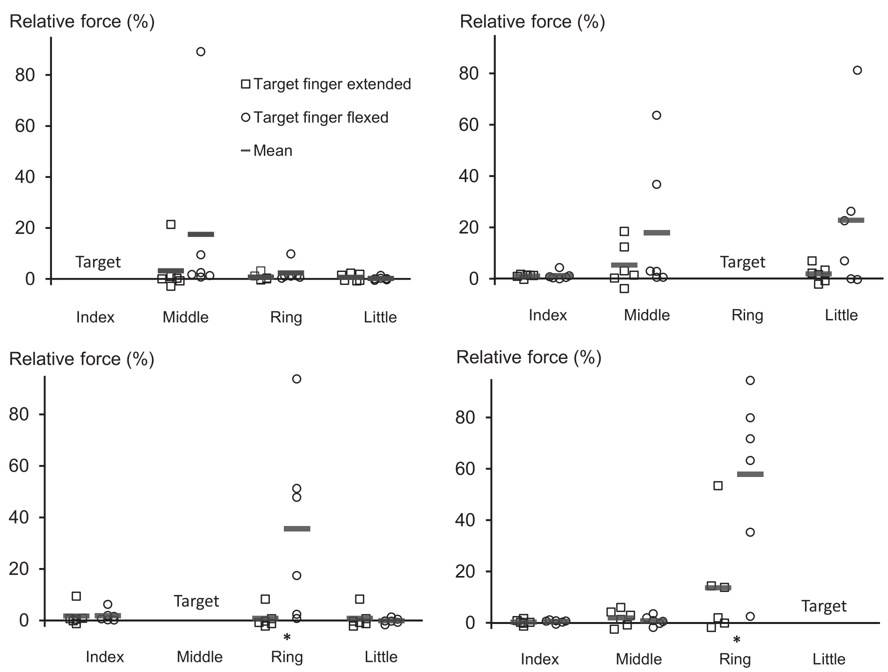

FIGURE 6 | Distribution of forces of flexor digitorum profundus to nontarget fingers upon the application of a 10 N load to the tendon corresponding to the target finger (Protocol B). The individual values ($n = 6$) and the mean of the relative force exerted by the nontarget fingers expressed as a percentage of the sum of forces by all fingers are shown. Significant ($p < 0.05$) differences between the two positions of the target finger (extended vs. flexed) are depicted with an asterisk at the bottom of the figure.

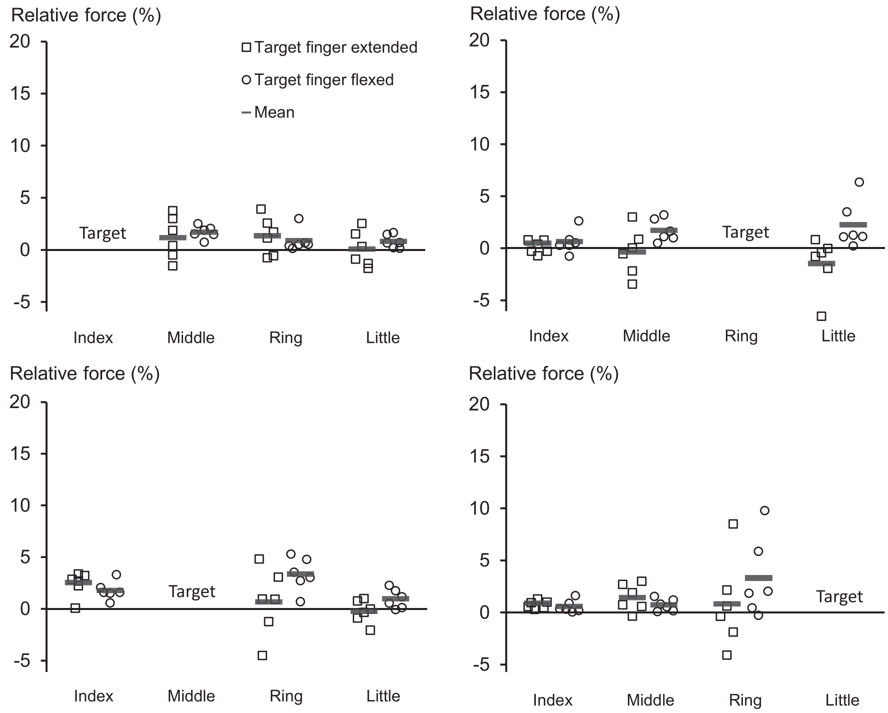

FIGURE 7 | Distribution of forces of flexor digitorum superficialis to nontarget fingers upon the application of a 10 N load to the tendon corresponding to the target finger (Protocol B). The individual values ($n = 6$) and the mean of the relative force exerted by the nontarget fingers expressed as a percentage of the sum of forces by all fingers are shown. No significant differences between the two positions of the target finger (extended vs. flexed) were found.

TABLE 2 | *F* and *p* values of mixed two-way ANOVAs to test for effects of target finger position (extended vs. 90° MCP flexion) on the relative force exerted by nontarget fingers (NTF).

		Index		Middle		Ring		Little	
	Factors and interactions	***F***	***p***	***F***	***p***	***F***	***p***	***F***	***p***
FDP	NTF	1.07	0.367	2.93	0.085	1.49	0.258	**14.00**	**<0.001**
	TF-position	2.06	0.172	4.26	0.057	4.36	0.054	**10.80**	**0.005**
	NTF × TF-position	1.63	0.229	**4.06**	**0.039**	1.27	0.310	**11.40**	**<0.001**
FDS	NTF	1.51	0.238	3.24	0.068	0.09	0.915	2.00	0.170
	TF-position	0.32	0.582	4.49	0.051	**13.17**	**0.002**	0.28	0.608
	NTF × TF-position	0.58	0.571	8.26	0.057	1.70	0.217	0.97	0.401

Note: Analysis has been done for each target finger (index, middle, ring, and little fingers) and flexor digitorum profundus (FDP) and superficialis (FDS) separately. A bold font depicts a significant main effect or interaction ($p < 0.05$).

nontarget fingers have been reported during passive single finger MCP joint movements [2]. In contrast, passive (i.e., hand anesthetized by ischemia) movements of a single DIP joint did not cause movements in the DIP joints of the nontarget fingers [23]. It should be noted that during movements of only the DIP joint, changes in length and relative position of the FDP compartment are much smaller than those during movements of the MCP or all joints [17, 24], most likely explaining this difference. The results of the present study can only be explained by musculoskeletal mechanisms, a likely mechanism being force transmission via connective tissue linkages between the tendons. However, interactions via the web space between fingers cannot be excluded. The web space consists of the soft tissue between bases of the fingers, including skin and subcutaneous tissue. It was also reported to affect finger independence in cadaveric hands, but only when fingers are hyperextended [12]. As the fingers in the present experiment were slightly flexed, the contribution of the web space to finger interactions was deemed minimal.

Previously, we reported for both young and older healthy subjects that during voluntary movements each of the fingers can move independently for some range [1, 25]. This was reported for the condition that the other, nontarget fingers were initially in an extended position, like in the present study. The range varied between fingers from about 20% of the total range of motion for the middle finger (i.e., a $\Delta\sum\Theta$ of about 33°) to about 60% for the index finger (i.e., a $\Delta\sum\Theta$ of about 93°). This large difference in range of independent movement with those found in the present study suggests that during voluntary movements finger independence is mediated also by other mechanisms. If during single finger movements the intertendinous connections of FDP and FDS are immediately involved, this means that (visually) independent finger flexion is possible only if the finger extensors of the nontarget fingers are activated, thereby, counteracting the exerted flexion forces. In agreement with this, we recently observed higher levels of activation of the extrinsic extensor muscles corresponding to the nontarget fingers than that of the target finger [26]. We therefore conclude that moving a single finger requires coactivation of finger flexors and extensors due to the mechanical effects of connective tissue connections between the tendons of extrinsic finger muscles, even in absence of observed motion of, or external forces exerted by the other fingers.

4.2 | Distribution of Forces Among FDP and FDS Tendons

With all four fingers in the extended position, we observed that a small portion of the applied forces (up to 14%) was transmitted to the nontarget fingers, particularly when loading the FDP tendons. Most force was transmitted to the fingers immediately adjacent to the target finger. These results agree with those found during static finger pressing [6, 7, 27, 28]. We recently investigated if the extent of interfinger dependency increases if fingers are moved relative to each other [7]. In such a case, the intermuscular [29, 30] and intertendinous connections are expected to tauten, become stiffer and, hence, transmit more force. In our study [7], we indeed found that forces exerted by the nontarget fingers increased as a function of target finger movement. Because this did not result in changes in the muscle activity in the muscle compartments corresponding to the nontarget muscles, the results were ascribed to mechanical connections. This conclusion is supported by the findings of the present study, that is, the distribution forces to nontarget fingers with all fingers extended increased in the condition that the target finger was flexed.

Whereas the portion of force distributed to nontarget fingers was substantial when loading FDP (Figure 6), it remained rather small for the FDS (Figure 7), even after changing the relative position of the target finger. This is in agreement with the description of anatomically dissecting FDS tendons, being removed from surrounding structures with little effort, versus that of FDP tendons, being tightly linked to synovial membranes [13]. These observations suggest that the mechanical effects of the connective tissue linkages between the FDS tendons are minimal.

4.3 | Limitations

All specimens were from older people. Previous studies have observed both increased [25, 31] as decreased finger interdependence [32] with aging, probably explained by differences in the task. For skin, contradictory changes in stiffness with aging have been reported [33]. The effects of aging on the intertendinous tissue properties of the extrinsic finger muscles are unknown, but since effects of age on tendon stiffness are limited [25, 34, 35], this factor appears to be of limited importance.

Freezing and thawing the arms may have affected the mechanical properties of the involved tissues. However, it has been shown that a limited number of freezing–thawing cycles (<3) does not affect the mechanical properties of human FDS and flexor pollicis longus tendons [36]. In the present study, we assumed that the same result applies to the other connective tissues in the hand.

Although we did find clear group effects, it should be noted that the sample size was low ($n = 6$) and the interindividual variability was high. The six hands varied greatly in the range of independent movement and distribution of forces. This is probably related to the variation in the presence and properties of the connective linkages between the tendons. Although not assessed in the present study, substantial interindividual variation has been reported for the intertendinous connections of FDP [13] and FDS [15]. A large sample size will be needed to assess if specific variations are encountered more frequently like those described for the FDS muscle bellies [10].

5 | Conclusions

We conclude that mechanical connections between the distal tendons of the FDS and FDP constrain independent control of the fingers. The mechanical effects of these connections is enhanced by moving one finger relative to the other fingers. The connections between the FDP transmit more force and, hence, appear to be stiffer than those of FDS.

6 | Perspective

Several functions have been attributed to the linkages between the tendons of the ED, such as spacing of the tendons and stabilization of the MCP joints [37]. Others have considered linkages between the muscle heads and tendons of extrinsic finger muscles as a cause of focal dystonia in musicians [16, 38] and the quadriga syndrome [14]. Changing the position of the middle, ring, and little fingers was shown to affect the activity level of several intrinsic and extrinsic hand muscles during a precision pinch task using only the index finger and thumb [39]. The authors conclude that surgeons and hand therapists should consider all fingers, and their connections, when restoring the function of a single finger.

There may also be conditions in which these linkages have functional advantages. In rock climbing, the pocket grip is used in case a hole does not fit all fingers. In such a case, the one or two active fingers are held in a relative extended position and it is commonly advised to flex the other fingers. The force exerted by one finger with the other fingers in a flexed position was found to increase by 20%–48% (depending on the DIP and PIP joint angles) compared with the condition in which all fingers were exerting force simultaneously [40]. This functional advantage of intermuscular and intertendinous linkages may also apply to other tasks in which not all fingers are used, such as throwing a fast ball or pinching. This raises the question if the advantages of this structural feature of our musculoskeletal system should also be exploited in the design of prosthetic and robotic hands. A first step may be to add these linkages to biomechanical models of the hand, which are currently consisting of fully isolated muscle-tendon units for each finger [24, 41–43].

Acknowledgments

We would like to thank Danny Koops and Loek Zwarekant for their help with building the frame for mounting the specimen, as well as Leon Schutte and Hans Agricola for providing technical assistance during the measurements.

Data Availability Statement

All individual data are included as Supporting Information.

References

1. J. C. van den Noort, N. van Beek, T. van der Kraan, et al., "Variable and Asymmetric Range of Enslaving: Fingers Can Act Independently Over Small Range of Flexion," *PLoS One* 11, no. 12 (2016): e0168636.

2. C. E. Lang and M. H. Schieber, "Human Finger Independence: Limitations Due to Passive Mechanical Coupling Versus Active Neuromuscular Control," *Journal of Neurophysiology* 92, no. 5 (2004): 2802–2810.

3. Z. M. Li, S. Dun, D. A. Harkness, and T. L. Brininger, "Motion Enslaving Among Multiple Fingers of the Human Hand," *Motor Control* 8, no. 1 (2004): 1–15.

4. C. Hager-Ross and M. H. Schieber, "Quantifying the Independence of Human Finger Movements: Comparisons of Digits, Hands, and Movement Frequencies," *Journal of Neuroscience* 20, no. 22 (2000): 8542–8550.

5. V. M. Zatsiorsky, Z. M. Li, and M. L. Latash, "Enslaving Effects in Multi-Finger Force Production," *Experimental Brain Research* 131, no. 2 (2000): 187–195.

6. K. Sanei and P. J. Keir, "Independence and Control of the Fingers Depend on Direction and Contraction Mode," *Human Movement Science* 32, no. 3 (2013): 457–471.

7. M. Mirakhorlo, H. Maas, and H. E. J. Veeger, "Timing and Extent of Finger Force Enslaving During a Dynamic Force Task Cannot be Explained by EMG Activity Patterns," *PLoS One* 12, no. 8 (2017): e0183145.

8. S. S. G. Dupan, D. F. Stegeman, and H. Maas, "Distinct Neural Control of Intrinsic and Extrinsic Muscles of the Hand During Single Finger Pressing," *Human Movement Science* 59 (2018): 223–233.

9. H. Van Duinen and S. C. Gandevia, "Constraints for Control of the Human Hand," *Journal of Physiology (London)* 589, no. 23 (2011): 5583–5593.

10. H. Maas, H. E. J. Veeger, and D. F. Stegeman, "Understanding the Constraints of Finger Motor Control," *Journal of Electromyography and Kinesiology* 38 (2018): 182–186.

11. H. P. von Schroeder and M. J. Botte, "Anatomy and Functional Significance of the Long Extensors to the Fingers and Thumb," *Clinical Orthopaedics and Related Research* 383 (2001): 74–83.

12. H. P. Von Schroeder and M. J. Botte, "The Functional Significance of the Long Extensors and Juncturae Tendinum in Finger Extension," *Journal of Hand Surgery* 18, no. 4 (1993): 641–647.

13. J. N. Leijnse, E. T. Walbeehm, G. J. Sonneveld, S. E. Hovius, and J. M. Kauer, "Connections Between the Tendons of the Musculus Flexor Digitorum Profundus Involving the Synovial Sheaths in the Carpal Tunnel," *Acta Anatomica* 160, no. 2 (1997): 112–122.

14. T. A. Schreuders, "The Quadriga Phenomenon: A Review and Clinical Relevance," *Journal of Hand Surgery, European Volume* 37, no. 6 (2012): 513–522.

15. J. S. Tan, L. Oh, and D. S. Louis, "Variations of the Flexor Digitorum Superficialis as Determined by an Expanded Clinical Examination," *Journal of Hand Surgery* 34, no. 5 (2009): 900–906.

16. J. N. Leijnse, "Measuring Force Transfers in the Deep Flexors of the Musician's Hand: Theoretical Analysis, Clinical Examples," *Journal of Biomechanics* 30, no. 9 (1997): 873–882.

17. M. Mirakhorlo, J. M. Visser, B. Goislard de Monsabert, F. Van der Helm, H. Maas, and H. Veeger, "Anatomical Parameters for Musculoskeletal Modeling of the Hand and Wrist," *International Biomechanics* 3, no. 1 (2016): 40–49.

18. A. Ghasemi and S. Zahediasl, "Normality Tests for Statistical Analysis: A Guide for Non-Statisticians," *International Journal of Endocrinology and Metabolism* 10 (2012): 486–489.

19. F. Frohse and M. Fränkel, *Die Muskeln des Menschlichen Armes* (Berlin: G. Fischer, 1908).

20. O. Ohtani, "Structure of the Flexor Digitorum Superficialis," *Okajimas Folia Anatomica Japonica* 56, no. 5 (1979): 277–288.

21. H. Maas and P. A. Huijing, "Myofascial Force Transmission in Dynamic Muscle Conditions: Effects of Dynamic Shortening of a Single Head of Multi-Tendoned Rat Extensor Digitorum Longus Muscle," *European Journal of Applied Physiology* 94, no. 5–6 (2005): 584–592.

22. H. Maas, R. T. Jaspers, G. C. Baan, and P. A. Huijing, "Myofascial Force Transmission Between a Single Muscle Head and Adjacent Tissues: Length Effects of Head III of Rat EDL," *Journal of Applied Physiology* 95, no. 5 (2003): 2004–2013.

23. S. L. Kilbreath and S. C. Gandevia, "Limited Independent Flexion of the Thumb and Fingers in Human Subjects," *Journal of Physiology (London)* 479, no. Pt 3 (1994): 487–497.

24. M. Mirakhorlo, N. Van Beek, M. Wesseling, H. Maas, H. E. J. Veeger, and I. Jonkers, "A Musculoskeletal Model of the Hand and Wrist: Model Definition and Evaluation," *Computer Methods in Biomechanics and Biomedical Engineering* 21, no. 9 (2018): 548–557.

25. N. Van Beek, D. F. Stegeman, I. Jonkers, C. L. de Korte, D. Veeger, and H. Maas, "Single Finger Movements in the Aging Hand: Changes in Finger Independence, Muscle Activation Patterns and Tendon Displacement in Older Adults," *Experimental Brain Research* 237, no. 5 (2019): 1141–1154.

26. N. van Beek, D. F. Stegeman, J. C. van den Noort, D. H E J Veeger, and H. Maas, "Activity Patterns of Extrinsic Finger Flexors and Extensors During Movements of Instructed and Non-Instructed Fingers," *Journal of Electromyography and Kinesiology* 38 (2018): 187–196.

27. V. M. Zatsiorsky, Z. M. Li, and M. L. Latash, "Coordinated Force Production in Multi-Finger Tasks: Finger Interaction and Neural Network Modeling," *Biological Cybernetics* 79, no. 2 (1998): 139–150.

28. S. L. Kilbreath, R. B. Gorman, J. Raymond, and S. C. Gandevia, "Distribution of the Forces Produced by Motor Unit Activity in the Human Flexor Digitorum Profundus," *Journal of Physiology (London)* 543, no. Pt 1 (2002): 289–296.

29. H. Maas, "Significance of Epimuscular Myofascial Force Transmission Under Passive Muscle Conditions," *Journal of Applied Physiology (1985)* 126 (2019): 1465–1473.

30. T. Finni, H. de Brito Fontana, and H. Maas, "Force Transmission and Interactions Between Synergistic Muscles," *Journal of Biomechanics* 152 (2023): 111575.

31. M. Mirakhorlo, H. Maas, and H. E. J. Veeger, "Increased Enslaving in Elderly Is Associated With Changes in Neural Control of the

Extrinsic Finger Muscles," *Experimental Brain Research* 236, no. 6 (2018): 1583–1592.

32. M. Shinohara, S. Li, N. Kang, V. M. Zatsiorsky, and M. L. Latash, "Effects of Age and Gender on Finger Coordination in MVC and Submaximal Force-Matching Tasks," *Journal of Applied Physiology (1985)* 94, no. 1 (2003): 259–270.

33. B. Lynch, H. Pageon, H. Le Blay, et al., "A Mechanistic View on the Aging Human Skin Through Ex Vivo Layer-by-Layer Analysis of Mechanics and Microstructure of Facial and Mammary Dermis," *Scientific Reports* 12, no. 1 (2022): 849.

34. C. Couppé, P. Hansen, M. Kongsgaard, et al., "Mechanical Properties and Collagen Cross-Linking of the Patellar Tendon in Old and Young Men," *Journal of Applied Physiology (1985)* 107, no. 3 (2009): 880–886.

35. C. C. Carroll, J. M. Dickinson, J. M. Haus, et al., "Influence of Aging on the In Vivo Properties of Human Patellar Tendon," *Journal of Applied Physiology (1985)* 105, no. 6 (2008): 1907–1915.

36. H. Huang, J. Zhang, K. Sun, X. Zhang, and S. Tian, "Effects of Repetitive Multiple Freeze-Thaw Cycles on the Biomechanical Properties of Human Flexor Digitorum Superficialis and Flexor Pollicis Longus Tendons," *Clinical Biomechanics (Bristol, Avon)* 26, no. 4 (2011): 419–423.

37. S. J. Chinchalkar, C. A. Barker, and B. Owsley, "Relationship Between Juncturae Tendinum and Sagittal Bands," *Journal of Hand and Microsurgery* 7, no. 1 (2015): 96–101.

38. J. N. Leijnse, "Anatomical Factors Predisposing to Focal Dystonia in the Musician's Hand—Principles, Theoretical Examples, Clinical Significance," *Journal of Biomechanics* 30, no. 7 (1997): 659–669.

39. S. Date, H. Kurumadani, K. Kurauchi, T. Fukushima, N. Goto, and T. Sunagawa, "Effect of Extension of the Ulnar Fingers on Force Control and Muscle Activity of the Hand During a Precision Pinch," *Journal of Hand Surgery, European Volume* 49 (2023): 608–616.

40. A. Schweizer, "Biomechanical Properties of the Crimp Grip Position in Rock Climbers," *Journal of Biomechanics* 34, no. 2 (2001): 217–223.

41. K. R. S. Holzbaur, W. M. Murray, and S. L. Delp, "A Model of the Upper Extremity for Simulating Musculoskeletal Surgery and Analyzing Neuromuscular Control," *Annals of Biomedical Engineering* 33, no. 6 (2005): 829–840.

42. F. D. Kerkhof, T. van Leeuwen, and E. E. Vereecke, "The Digital Human Forearm and Hand," *Journal of Anatomy* 233, no. 5 (2018): 557–566.

43. L. Engelhardt, M. Melzner, L. Havelkova, et al., "A New Musculoskeletal Any Body Detailed Hand Model," *Computer Methods in Biomechanics and Biomedical Engineering* 24 (2020): 777–787, https://doi.org/10.1080/10255842.2020.1851367.

Supporting Information

Additional supporting information can be found online in the Supporting Information section.